EVALUATION OF INFRARED IMAGES BY USING A HUMAN THERMAL MODEL

N. Kakuta[1], S. Yokoyama[2], T. Suzuki[1], T. Saito[1], and K. Mabuchi[1]

[1]Center for Collaborative Research, The University of Tokyo, 4-6-1 Komaba, Meguro-ku, Tokyo, 153-8904 Japan

[2]Graduate School of Engineering, Hokkaido University, Kita-13, Nishi-8, Kita-ku, Sapporo, 060-8628 Japan

Abstract- **In order to evaluate IR images obtained under various thermal environmental conditions, we proposed a human thermal model that can be used for converting IR images into those under a standard condition. The developed model was based on a numerical calculation of bio-heat transfer equations that express heat transfer phenomena within the human body and a mathematical model of the thermoregulation system. A comparison of an IR image which was converted under the standard condition (30˚C) with the original one at 30˚C indicated that the method using our model was effective to eliminate the influence of the thermal environmental condition.**

Keywords- **Infrared image, human thermal model, thermal environmental condition, image conversion**

I. INTRODUCTION

It is useful to develop a method to obtain an objective standard to evaluate the skin surface temperature distribution. If there were such a method, thermographers would use it in combination with conventional subjective diagnosis. Normalizing or averaging skin surface temperature distributions by means of acquiring enormous amounts of experimental data seems to have an inherent limitation. We have developed a human thermal model that simulates the heat transfer phenomenon within the body and predicts the internal temperature, including the skin surface temperature [1,2]. We first applied the model to comparing images under various thermal environments. Skin surface temperature is greatly influenced by thermal environmental conditions. Therefore, in order to detect and evaluate an abnormal area from IR images, eliminating this influence is required [3]. When comparing two thermal infrared (IR) images under different thermal environmental conditions, for example, it is necessary to be able to convert one image into that under the same condition as the other or to convert two images into those under a standard thermal environmental condition. This article presents the outline of our human thermal model and the IR images converted from those under another thermal environmental condition.

II. HUMAN THERMAL MODEL

A. Bio-Heat Transfer Equations

The bio-heat transfer equations that we adopted are

summarized in Table 1. The second term on the right hand in Equation (1) shows the heat exchange through the capillaries between the entering arterial blood and the tissue. The third and the fourth terms show the heat transmission through the large vessels between the tissue and the arterial blood and the tissue and the venous blood, respectively. The fifth term, M, represents the metabolic heat production rate. Equations (2) and (3) are heat transfer equations for the arterial and venous circulatory system, respectively. The first terms on the right hand in both equations show the heat transfer from the blood in an adjacent system or adjacent region to the present blood system. The second term shows the heat exchange between the blood and the neighboring tissue. The third term expresses the countercurrent heat exchange between the artery and vein.

TABLE I
BIO-HEAT TRANSFER EQUATIONS

Tissue

$$\rho(\boldsymbol{r})c(\boldsymbol{r})\frac{\partial T(\boldsymbol{r},t)}{\partial t} = \nabla \cdot \lambda(\boldsymbol{r})\nabla T(\boldsymbol{r},t) + \frac{f(\boldsymbol{r},t)c_b}{V}[T_{ab}(\boldsymbol{r},t) - T(\boldsymbol{r},t)] \quad (1)$$

$$+ H_{ab}(\boldsymbol{r},t)[T_{ab}(\boldsymbol{r},t) - T(\boldsymbol{r},t)] + H_{vb}(\boldsymbol{r},t)[T_{vb}(\boldsymbol{r},t) - T(\boldsymbol{r},t)] + M(\boldsymbol{r},t)$$

Arterial blood pool

$$\rho_b c_b V_{ab}(\boldsymbol{r},t)\frac{\partial T_{ab}(\boldsymbol{r},t)}{\partial t} = f_{ab}(\boldsymbol{r},t)c_b [T_{am}(\boldsymbol{r},t) - T_{ab}(\boldsymbol{r},t)] \quad (2)$$

$$+ \iiint_V H_{ab}(\boldsymbol{r},t) [T(\boldsymbol{r},t) - T_{ab}(\boldsymbol{r},t)]dV + H_{av}(\boldsymbol{r},t) [T_{vb}(\boldsymbol{r},t) - T_{ab}(\boldsymbol{r},t)]$$

Venous blood pool

$$\rho_b c_b V_{vb}(\boldsymbol{r},t)\frac{\partial T_{vb}(\boldsymbol{r},t)}{\partial t} = f_{vb}(\boldsymbol{r},t)c_b [T_{vn}(\boldsymbol{r},t) - T_{vb}(\boldsymbol{r},t)] \quad (3)$$

$$+ \iiint_V \left[\frac{f(\boldsymbol{r},t)c_b}{V} + H_{vb}(\boldsymbol{r},t)\right][T(\boldsymbol{r},t) - T_{vb}(\boldsymbol{r},t)]dV + H_{av}(\boldsymbol{r},t)[T_{ab}(\boldsymbol{r},t) - T_{vb}(\boldsymbol{r},t)]$$

Heat transfer between body surface and environment

$$q_s = q_c + q_r + q_{eva} + q_d \quad (4)$$

t: time [s], $\boldsymbol{r}$: coordinates vector in tissue, T: temperature [K], q: heat flux [W/m^2], ρ: density [kg/m^3], c: specific heat [J/(kg·K)], λ: thermal conductivity [W/(m·K)], f: blood flow rate [kg/s], V: volume [m^3], M: metabolic heat production rate [W/m^3], H: heat transfer coefficient [W/(m^3·K)], H_{av}: heat transfer coefficient between artery and vein for countercurrent flow [W/K], q_c: convective heat transfer rate [W/m^2], q_r: radiant heat transfer rate [W/m^2], q_{eva}: evaporative heat transfer rate [W/m^2], q_d: conductive heat transfer rate [W/m^2].
Subscripts- b: blood, ab: arterial, vb: venous, am: adjacent arterial system, vn: adjacent venous system, s: skin surface.

B. Geometric Model of the Human Body

We adopted a 16-cylinder-segment model as the geometric model of the body (Fig. 1 (a)). Each segment was divided into concentric layers (Fig. 1 (b)). We assumed that the properties of each layer are

Report Documentation Page

Report Date 25OCT2001	Report Type N/A	Dates Covered (from... to) -

Title and Subtitle Evaluation of Infrared Images by Using a Human Thermal Model	Contract Number
	Grant Number
	Program Element Number

Author(s)	Project Number
	Task Number
	Work Unit Number

Performing Organization Name(s) and Address(es) Center for Collaborative Research, The University of Tokyo, 4-6-1 Komaba, Meguro-ku, Tokyo, 153-8904 Japan	Performing Organization Report Number

Sponsoring/Monitoring Agency Name(s) and Address(es) US Army Research, Development & Standardization Group (UK) PSC 802 Box 15 FPO AE 09499-1500	Sponsor/Monitor's Acronym(s)
	Sponsor/Monitor's Report Number(s)

Distribution/Availability Statement
Approved for public release, distribution unlimited

Supplementary Notes
Papers from the 23rd Annual International Conference of the IEEE Engineering in Medicine and Biology Society, October 25-28, 2001, held in Istanbul, Turkey. See also ADM001351 for entire conference on cd-rom., The original document contains color images.

Abstract

Subject Terms

Report Classification unclassified	Classification of this page unclassified

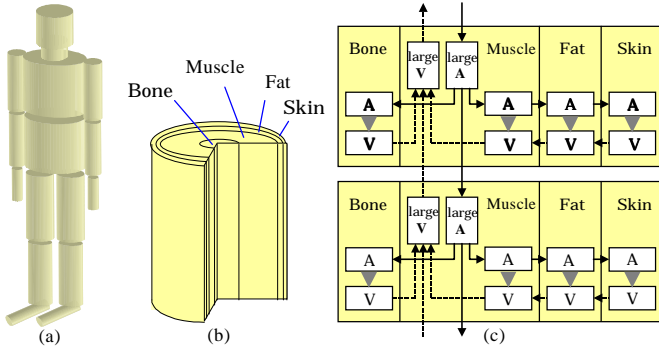| Classification of Abstract unclassified	Limitation of Abstract UU

Number of Pages
4

Fig.1. (a) 16-cylinder-segment model. (b) Concentric multi-layered model for the extremities. The head, neck, thorax, and abdomen segments have internal organ layers. (c) Schematic of the blood circulatory system model. Symbols A and V represent the arterial and venous blood pools, respectively. In one segment, there is a pair of the large arterial and venous blood pools corresponding to the main artery and vein. The large blood pool is connected to one in adjacent segment each other. In each layer, there is a pair of arterial and venous blood pools corresponding to the arteriole, venules, and capillaries.

homogeneous and did not take into account the longitudinal and angular coordinates. In a segment, there are a large arterial blood pool and a venous blood pool corresponding to the main artery and the main vein, respectively (Fig. 1 (c)). Heat transfer between two segments occurs through the large blood pools.

C. Skin Blood Flow Regulation

A human thermal model needs to include a program for skin blood flow regulation. We proposed the equation for skin blood flow rate [4]. The skin blood flow rate of each segment was renewed with each calculation of the bio-heat transfer equations.

D. Calculated Results of Body Temperature

The developed computer program simultaneously calculates the distributions of internal temperature, heat flux, and blood temperature of all segments with time by inputting thermal environmental factors such as air temperature, mean radiant temperature, air velocity, and relative humidity of each segment.

Fig. 2 shows the results simulated under the condition that both the air temperature and the mean radiant temperature were changed from 30°C to 24°C at 60 min. As can be seen, the skin surface temperatures had the characteristics of each segment, that is, the temperatures of the peripheral segments were lower. The calculated temperatures at the center of the head and abdomen, which correspond to the hypothalamus and rectum, respectively, were adequate values [5]. Fig. 2 (c) demonstrates that the temperature descent rates differed among the segments, chiefly because their thermal capacities and metabolic heat production rates differed. The diminution of the core temperature (hypothalamus
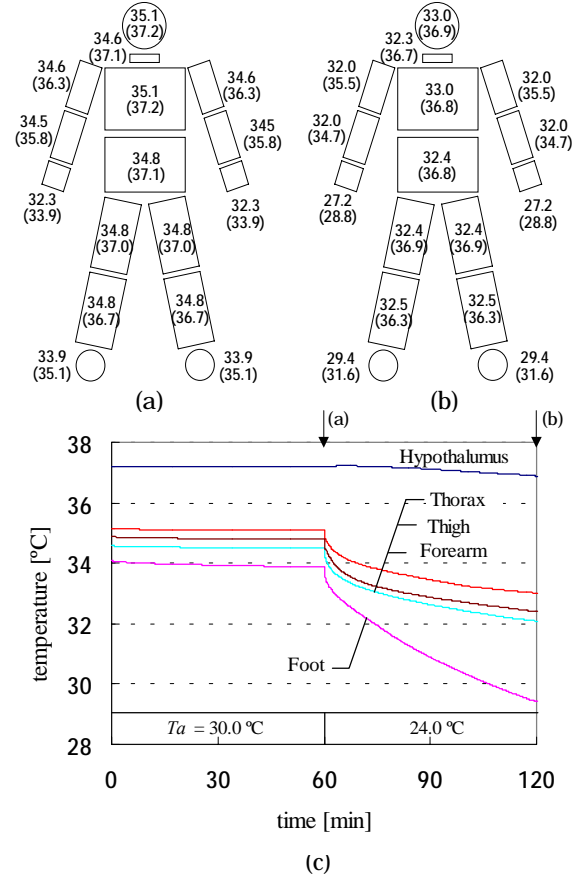

Fig.2. Simulated body temperature profile. Air temperature and mean radiant temperature were 30°C for 0-60 min and changed to 24°C at 60 min. They were maintained at 24.0°C during subsequent 60-min period. Air velocity and relative humidity were set to be 0.1m/s and 50.0 %, respectively. (a) Skin surface temperatures at 60 min. (b) Skin surface temperatures at the end (120 min). The values in parentheses are temperatures at the center of the segments. (c) Hypothalamus temperature (temperature at the center of the head) and skin temperatures of four segments with time.

temperature) was 0.3°C at 120 min. That value was smaller than that of the skin surface temperature.

III. CONVERTING INFRARED IMAGES

### A. Method for Converting Infrared Images

First, the image of an objective segment such as the hand, forearm, or calf is picked out. Meanwhile, making use of our human thermal model, the difference (offset) between the skin surface temperatures under the thermal environmental condition and under the standard condition is calculated. Next, the intensity corresponding to this offset is added to or subtracted from the pixel intensity of the original image.
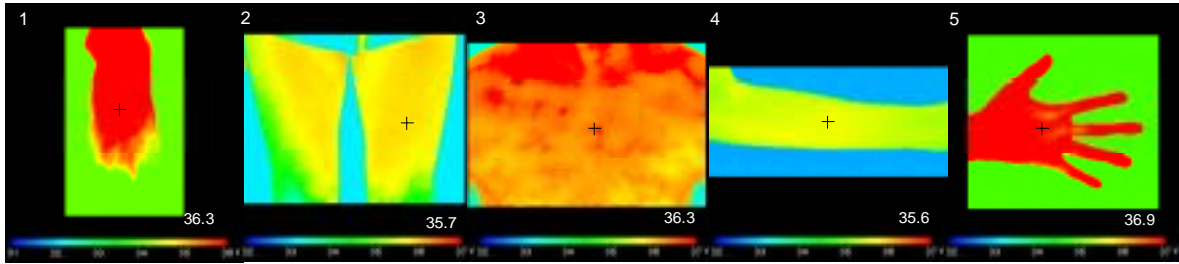
B. Converted Images

The IR images shown in Fig. 3 are experimental results obtained from one of the participating healthy Japanese
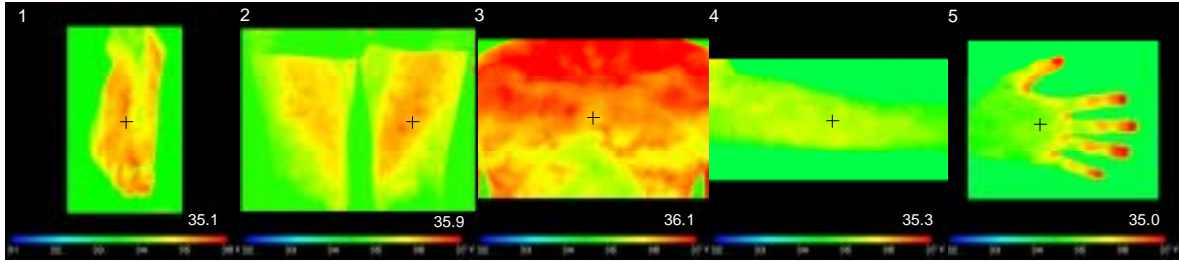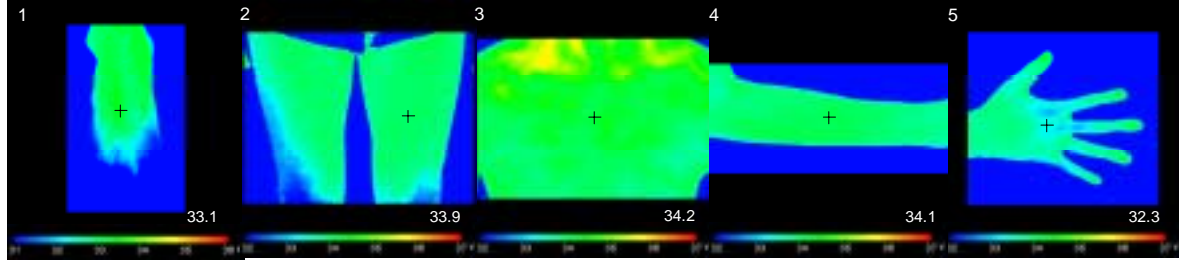
Fig.3. IR images of 1: the top side of the foot, 2: the front of the thigh, 3: the chest, 4: the forearm, and 5: the back of the hand under the condition of 30˚C air temperature for 60 min (a) and subsequently 26˚C for 60 min (b). The images in the bottom row (c) are those converted from the images in (b) into those at 30˚C. The temperature color legend of the same scale is used in (a), (b), and (c) (1: 31.0-36.0˚C; 2-5: 32.0-37.0˚C). The numeric in the image represents the temperature at the symbol '+'.

males who wore only shorts and were asked to rest in the sitting position in the test room. The duration and the time to change the air temperature were the same as those shown in Fig. 2 (c). Fig. 3 (a) displays the IR images at 30˚C acquired at the elapsed time of 60 min. The air temperature was changed by a step pattern to 26˚C and kept for 60 min. The images at 26˚C were acquired at the total elapsed time of 120 min (Fig. 3 (b)) and converted into those at 30˚C by the calculated offsets (Fig. 3 (c)). The relative humidity was fixed at 50 % throughout all experiments.

In Fig. 3, it is obvious that the whole temperature of the converted image approximates the original image at 30˚C more than the original one at 26˚C. The offsets used for converting the images of the foot, thigh, chest, forearm, and hand were 3.3, 1.9, 2.1, 1.6, and 3.6˚C, respectively. The image of the chest in Fig. 3 (a) is similar to that in Fig. 3 (c). The temperature inhomogeneity

within peripheral segments such as the hand and the foot increased along with a decrease of the air temperature; for example, the finger temperature at 26˚C is noticeably lower than that in other parts of the hand because the vasoconstriction of a finger is the most sensitive and the volume (thermal capacitance) of a finger is small. Furthermore, the temperatures of the foot and the hand in Fig. 3 (c) are higher than those at 30˚C (Fig. 3 (a)), which means that the calculated offset exceeded the real temperature difference. The converted images of the thigh and the forearm are in relative agreement with the original ones at 30˚C.

IV. DISCUSSION

The whole temperatures of the converted IR images approximated the original ones at 30˚C to some degree. At first glance, the 16-cylinder-segment model is a rough

geometric model. Nevertheless, as seen in Fig. 2, the calculated results of the core temperature and the skin surface temperatures in the neutral zone compared well with the realistic temperature profiles, which indicates that relatively adequate properties could be assigned to each segment. The converted image of the chest had been expected to agree with the original one because the trunk has a large thermal capacity, the individual variation is relatively small, and vasoconstriction in the skin is slight. In fact, there was little difference between the temperature of the converted image of the chest and the original one, as shown in Fig. 3. Although we cannot claim the validity of our model only from the results of the chest, we should regard such a region important to evaluate the skin surface distribution of the body because its skin surface temperature can be precisely simulated. That is, its temperature could be used as a standard to normalize the skin temperature distribution or to produce an index comparing the level of vasoconstriction in the skin of each segment.

Considering the factors that caused the discrepancy, the results of the other segments could be modified immediately. First of all, changing the physiological properties, such as the parameters of skin blood flow regulation and the metabolic heat production rates, can have an immediate effect. While admitting that IR imaging can hardly be performed under a severe condition, these properties should be investigated by using novel technologies. However, for some segments whose skin surface temperatures vary with subjects, e.g., the hand and the foot, we should notice that it is not very worthwhile to make the converted image agree with the original one. As well as the properties, it is necessary to improve the geometry of the model. Since the sizes of the geometric model were constant throughout the calculations, it seems effective to change the sizes for those of each subject. In addition, computer graphics technology or a laser scanning system can easily create a body surface model. Although geometric models that resemble the body form better than a cylinder-segment model have been used [6], constructing a detailed geometry of the tissue containing vessel networks is the subject for the future.

The skin surface temperature depends on not only the thermal environment at that time but also its history. A thermographer asks a subject to rest for a certain time (more then 20 min recommended) before the thermographic examination takes place. However, even if this method were performed, the body temperature would not become stable within such a short period. In using the human thermal model, the input factors of the thermal environment should be a function of time. Except for an experiment in a test room with sufficient duration, actually, there are few or no cases in which experimental data of thermal environmental history have been recorded. In this case, the thermal environmental history could be estimated from the behavior of a subject until then or the core temperature, which might reflect the thermal environment. The core temperature also interacts with the physiological condition history. We must investigate the relationship between the reliability of the model and the degree of precision of each input factor: the thermal environmental history and physiological condition history.

An advantage of the evaluation of IR images using the thermal model is to provide common information to all researchers. In particularly, it is possible to quantify the effect of a certain factor on the skin surface temperature. Then, researchers can quantitatively analyze an IR image making use of the various calculated results. In this study, the calculated results were applied to eliminate the influence of the thermal environment, which suggested that the human thermal model can cover numerous applications.

REFERENCES

[1] N. Kakuta, S. Yokoyama, and K. Mabuchi, "Development of a human thermal model and its applications for thermographic diagnosis," *Proc 1st Joint BMES/IEEE EMBS Conf.*, p. 1103, Atlanta, 1999.
[2] S. Yokoyama, N. Kakuta, and K. Ochifuji, "Development of a new algorithm for heat transfer equation in the human body and its applications," *Appl. Human Sci,* vol. 16, no. 4, pp. 153-159, 1997.
[3] K. Mabuchi, T. Chinzei, I. Fujimasa, S. Haeno, K. Motomura, Y. Abe, and T. Yonezawa, "Evaluating asymmetrical thermal distributions through image processing," *IEEE Eng. Med. Biol. Mag.*, vol. 17, no. 4, pp. 47-55, 1998.
[4] S. Yokoyama, N. Kakuta, T. Togashi, Y. Hamada, M. Nakamura, and K. Ochifuji, "Development of prediction computer program of whole body temperatures expressing local characteristic of each segment, part 2- Analysis of the mathematical model for the control of skin blood flow," *Trans. SHASE Japan*, vol. 78, pp. 1-8, 2000 (in Japanese).
[5] P. Webb, "Temperatures of skin, subcutaneous tissue, muscle and core in resting men in cold, comfortable and hot conditions," *Euro. J. Appl. Physiol.,* vol. 64, pp. 471-476, 1992.
[6] J. Werner, M. Buse, and A. Foegen, "Lumped versus distributed thermoregulatory control: Results from a three-dimensional dynamic model," *Biol. Cybern.,* vol. 62, pp. 63-73, 1989.
[7] H. Arkin, L. X. Xu, and K. R. Holmes, "Recent developments in modeling heat transfer in blood perfused tissues," *IEEE Trans. Biomed. Eng.*, vol. 41, no. 2, pp. 97-107, 1994.
[8] N. Kakuta, S. Yokoyama, M. Nakamura, and K. Mabuchi, "Estimation of radiative heat transfer using a geometric human model," *IEEE Trans. Biomed. Eng.*, vol. 48, no. 3, pp. 324-331, 2001.